International Journal of Science and Research Archive
eISSN: 2582-8185
Cross Ref DOI: 10.30574/ijsra
Journal homepage: https://ijsra.net/

(REVIEW ARTICLE)

Check for updates

Deep ensemble learning for chickenpox detection from clinical images

Seyyed Kamran Hosseini [1,*], Faraidoon Habibi [2] and Naqibullah Vakil I [2]

[1] *Department of Software Engineering, Computer Science Faculty, Herat university, Herat, Afghanistan.*
[2] *Department of Network Engineering, Computer science Faculty, Herat University, Herat, Afghanistan.*

International Journal of Science and Research Archive, 2024, 12(01), 344–352

Publication history: Received on 23 March 2024; revised on 03 May 2024; accepted on 06 May 2024

Article DOI: https://doi.org/10.30574/ijsra.2024.12.1.0771

Abstract

Chickenpox caused by the varicella-zoster virus is an extremely contagious viral infection common in children and quickly develops into a severe problem. Over 90% of unvaccinated people have been infected. Still, infection occurs at different ages in different parts of the world- Over 70 % of people become infected by the age of 10 years in the United States, the United Kingdom, and Japan, and by the age of 20 in India, West Indies, and South East Asia. Automatic classification of the specific disease is a challenging task to present clinicians to distinguish between different kinds of skin conditions and recommend suitable treatment. Convolutional Neural Networks have recently achieved great success in many machines learning purposes and have presented a state-of-the-art performance in various computer-assisted diagnosis applications. This study proposes a deep neural network-based method that follows an ensemble approach by combining VGG-16, VGG-19, and ResNet-50 architectures to distinguish chickenpox from other skin conditions. Experimental test results have achieved accurate classification with an assuring test accuracy up to 93%.

Keywords: Chickenpox; Ensemble; Classification; Deep Learning; Convolution Neural Network

1. Introduction

Infectious disease occurs when a pathogen infects a person from another person or an animal. It harms individuals and causes harm on a macro scale and, therefore, is regarded as a social problem [1]. The recognition of infectious diseases through the analysis of clinical images can provide timely and accurate background knowledge for implementing preventative measures, such as promoting and monitoring the effectiveness of vaccination campaigns [2].

Chickenpox, also known as varicella, caused by the varicella-zoster virus (VZV), is a highly contagious disease that causes an itchy, blister-like rash. It is transmitted through direct contact or by directly touching the infected person's inflammation, saliva, mucus, or droplet. The incubation time for chickenpox ranges from 11 to 21 days. At first, you might feel a bit feverish, have a headache, feel restless, or lose your appetite. On the following day, the characteristic lesions begin to appear on the body. The blister evolves to form small bumps and then changes to vesicles. Over the next several days, the blisters rupture and then crust [3]. The rash may begin on the chest, back, or face before spreading across the body, including inside the mouth, eyelids, or].

Over 90% of unvaccinated people become infected. Still, infection occurs at different ages in different parts of the world. In the United States, United Kingdom, and Japan, over 80% of people are infected by the age of ten, while in India, Southeast Asia, and the West Indies, infection occurs between the ages of 20 and 30 [4]. Chickenpox is extremely contagious disease in children under the age of two. In fact, young children account for 90% of all cases. However, teenagers and adults can get it as well [6]. Encephalitis, pneumonia, and skin infection are some of the problems associated with chickenpox; some of these complications can result in the patient's death. Moreover, chickenpox can potentially cause severe complications in pregnant women, resulting in congenital disabilities in the baby. Chickenpox

* Corresponding author: Seyyed Kamran Hosseini

consequences are more likely in people who have compromised immune systems. It would be ideal to have a method for detecting chickenpox vesicles early on, especially in adults [3].

Although the rash typically disappears in two to four weeks, some individuals have nerve discomfort that lasts months or years. Herpes zoster, often known as shingles or zona, is the name given to this condition. It's also helpful to have a tool that can tell the difference between chickenpox, normal images, and other infectious diseases.

This paper aims to develop a model capable of detecting chickenpox rash and analyzing and distinguish it from other infectious diseases. In the long run, it is intended to become a part of a general tool designed to assist physicians and patients alike in diagnosing skin diseases. A method capable of chickenpox blisters characterization can be used in many fields. Besides phone application, which is particularly required in developing countries where health workers are scarce, it can also be deployed in telemedicine to facilitate the recognition of chickenpox or airport security to prevent transmission of the disease.

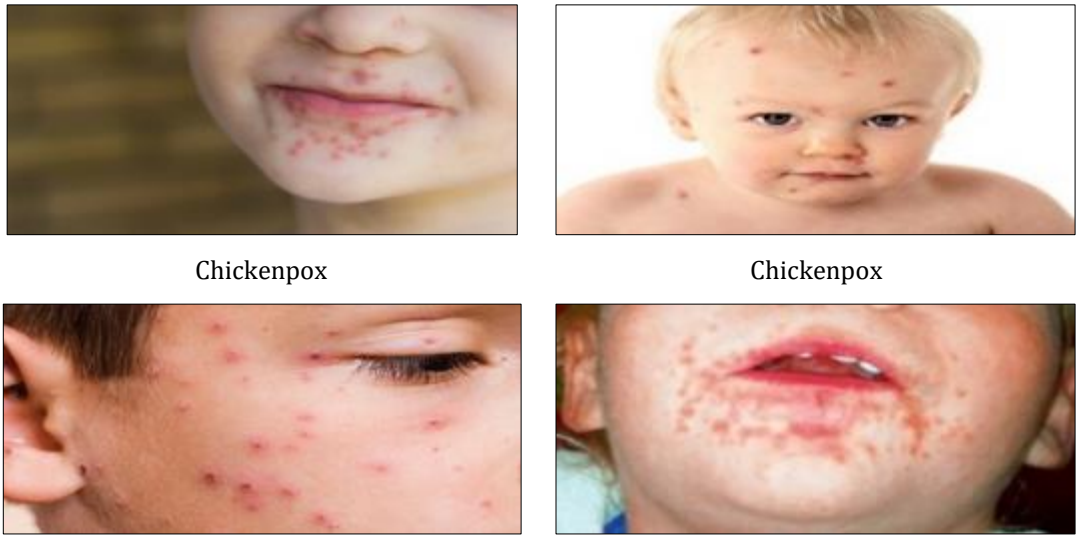

Figure 1 Sample images of chickenpox and non-chickenpox

The rest of the paper is organized as follows. In the first section, we discuss related work. Our dataset, ensemble approach, and experimental setup are presented in Section 3, followed by results and an evaluation of misclassifications. Sections 4 present discussion, conclusions and propose future work.

2. Related work

In this section, the emphasis is on applying various skin diseases detection and diagnosis methods, with more focus on the recent researches that have used deep learning for the same purpose.

Recent advances in AI have made deep CNN the go-to model for virtually every image-related problem. As a class of deep learning algorithms, deep CNN is made of stacks of processing layers, which allow it to learn complex features hierarchically from visual data. With the state-of-the-art performance in image processing, CNN has been used increasingly widely to classify, detect, and diagnose skin diseases.

Early diagnosis and treatment of chickenpox can reduce the damage caused by this infection. However, the skin disease identification accuracy is unideal due to the similarity between different skin rash and the limited number of dermatologists and experts with professional knowledge. So, the classification of skin conditions has become a serious scientific challenge. To address the issue of skin rash diagnosis and treatment, people applied computer-aided diagnosis for automatic skin rash recognition based on the skin disease images earlier [7]. Many specialists and scholars have been engaged in the image identification of skin conditions. Recently published articles by Dick et al. are a good starting point. This article lists the relevant articles on the diagnosis of melanoma in deep learning [8]. This research investigates the studies status of skin rash recognition in recent years, summarizes the datasets used by works, and investigates image preprocessing, data augmentation, deep learning model, and framework performance indicators. On the one

hand, this study gives a reference for deep learning techniques for dermatologists. Also, this work facilitates studies to quickly and accurately retrieve the literature related to skin disease recognition. This survey's foundation is the quickly developing artificial intelligence-based (AI) diagnosis technology in the medical field, becoming increasingly popular among researchers.

Furthermore, many models and tools have been built to help these professionals in their task of detecting diseases in many fields [9, 10, 11, 12, 13]. This has proven to add more reliability and confidence to specialists in their practices as they have more information to diagnose patients. For dermatology and skin diseases, detection has not been different. History reveals that many methods had been made for years, applications with shallow models such as Support Vector Machines (SVM) [15] and K-Nearest Neighbors (KNN) [14] had been proven to achieve a state-of-the-art performance but are as well tiresome to create applications that involve such approaches. Seeing this, some works have been applying this method to classifying skin disease with success. One common challenge in this domain is the lack of quality and scarcity of open datasets. It is common to see studies with only a couple hundred examples. This is a characteristic of the medical field. Many hospitals hold vast amounts of data and do not make it public mainly because of patient privacy issues and ethics. However, many authors still push forward the technology in such fields, overcoming these challenges. For this work, we listed some related studies that use deep learning in dermatology, applying neural networks to skin disease.

Matsunaga et al. [16] proposed a method to classify seborrheic keratosis, melanoma, and nevocellular nevus, utilizing dermoscopic images. In this research, they proposed an ensemble approach solution with two binary models that still leveraged the patients' age and sex information, if they were available. Moreover, they used methods of data augmentation, using a combination of 4 transformations (translation, rotation, flipping, and scaling and). For the architecture, they preferred the ResNet-50 implementation on the framework Keras, with personal modifications. This classifier was pre-trained with the weights for a generic object recognition model and finally used two optimizers AdaGrad and RMSProp. This study was then submitted to the ISBI Challenge 2017 and won first place, ahead of the other 22 competitors.

Nasr-Esfahani et al. [17] presented a CNN-based melanoma diagnosis method that applies a preprocessing step to adjust the illumination, segment the images, and improve the images through a Gaussian filter. This technique achieved an accuracy of 81%. Majtner et al. [18] proposed a method that automatically recognizes melanomas; in their system, the descriptor vector of each image is acquired utilizing RSurf, Local Binary Patterns (LBP), and Convolutional Neural Networks. Additionally, they use the method Support Vector Machines (SVM) for classification. During training, they utilized 900 images and 379 for testing. The highest accuracy achieved by the authors was of 82.6%.

Kwasigroch et al. [19] present a similar solution to the previous 3. This is because this domain faces inherent limitations and challenges, particularly with data scarcity. This work applies transfer learning, using two different learning models, ResNet-50 and VGG19, both pre-trained on the ImageNet dataset. These were used to distinguish between benign and malignant lesions using 10,000 dermoscopic images. For the accurate learning process, also applied up-sampling for underrepresented classes. This process was done using a random number of transformations, such as rotation, zooming, shifting, and flipping. Furthermore, this work presented three experiments, first with the VGG-19 architecture with two extra convolutional layers, two fully connected layers, and one neuron with a sigmoid function. Second, it experimented with the ResNet-50 classifier and finally implemented a VGG-19 as the fully connected layer with an SVM classifier. As a final result, the modified implementation of the VGG-19 had the best results. However, the main reason for the poor results in the ResNet50 model was the small amount of training data. Maybe it would be possible to train a small model with vast amounts of data and produce better results.

There are several studies using digital images. For example, a study [20] highlights the ability of his DLS to assist doctors in diagnosing skin diseases. DLS consists of two main components. A variable number of deep convolutional neural network modules that process a flexible number of input images, and shallow modules that process metadata such as demographics and historical medical information. DLS has been shown to play an effective role in the differential diagnosis of skin diseases and can improve the accuracy of general practitioners' performance. [21] Additionally, three skin diseases (melanoma, eczema, and psoriasis) have been described. We acquire a digital image of the pathologically affected skin region and preprocess it to extract features using a pre-trained technique (CNN) (Alex-Net) and SVM. The study succeeded in detecting 4,444 diseases in three different types with a 100% cure rate. In a study [22] discussing skin disease, digital images of the affected skin area were created. Computer technology was used to analyze, process, and distribute image data based on various characteristics of the images. Using complex techniques such as (CNN), the features are extracted and the image classifier is based on the SoftMax classifier algorithm, and the re-diagnosis is obtained as output. In summary, the system is more accurate and can provide faster results. A study [23] detected 4,444 skin diseases using computer vision-based techniques. We used multiple image processing algorithms and fed them into

a artificial neural network to train the data. There are two phases. First, we preprocess the skin color to extract features. Second: Detection of 9 types of related diseases. Next, an image processing algorithm is applied to the image of the infected area. It then uses user input such as gender, age, duration, and type of training fluid. It is difficult to analyze the skin surface using image processing technology. However, in this study, he collected 4,444 good patient samples for training, and the detection rate results showed that he was very successful in detecting 9 diseases. The use of deep learning techniques to diagnose skin diseases is discussed in [24]. Due to rare skin diseases and the similarity of skin diseases, it is difficult to obtain data and use them for training. In this study, a deep learning convolutional neural network and a skin feature representation CNN model were used to detect skin diseases in images. This study showed that deep learning performs very well compared to other prior techniques such as histograms, statistics, and color textures.

Moreover, a recent study presented a Mobile Net algorithm to distinguish seven skin conditions and rashes [25]. Interestingly, chickenpox rash was among their seven skin diseases. But the evidence (and accuracy) of measles identification was not reported by the developers. To the best of our knowledge, the only published research in the area of varicella is paper by Oyola et al. [3]. The authors proposed a solution through color transformation, equalization, and edge detection by applying the image processing method. The images of varicella were eventually collected and classified through Hough transform. The final empirical results demonstrated that a better diagnosis was received in detecting varicella, and a preliminary test was also conducted on varicella and herpes zoster on that basis. Apart from these works, we are not aware of other studies for chickenpox rash classification.

3. Material and Architecture

3.1. Data Collection

As there are no public resources available that contain a vast library of chickenpox images, we gathered the images for our work applying the Bing Web Search API (Microsoft Azure package) to parse images from the public source. The images we collected contain rash images of 11 different disease states: Bowen's disease, dermatofibroma, eczema, enterovirus, keratosis, measles, psoriasis, ringworm, HFMD and scabies. Additionally, images of normal skin are also included in the data set. In total, there are 205 images of the chickenpox rash and 1168 non-chickenpox images present in the dataset [8]. Additionally, images of normal skin are also included in the data set. Table I present the complete list of the images we collected.

Table 1 Distribution of image samples

Disease	Number of Images
Measles	112
Eczema	23
Erythema	103
Urticaria	77
Lupus	68
Bowen's Disease	109
Scabies	211
Psoriasis	115
Impetigo	86
Atopic Dermatitis	109
Ringworm	125
Keratosis	96
Dermatofibroma	65
HFMD	236
Normal	347
Total	2192

3.2. Proposed Method

This work investigates the performance of VGG-16, VGG-19, and ResNet-50 architectures separately and their ensemble (the combined architectures) for chickenpox classification. VGG-16 and VGG-19 both have the same concept of extracting the features in the convolutional layers. The high-level reasoning in the neural network and the classification step are done utilizing the fully connected layers. We have adjusted the fully connected layers in all architectures to output 2 classes instead of 1000 classes proposed for ImageNet.

3.3. Clinical identification of skin diseases

Currently, the types of images detected in the field of skin disease detection are relatively uniform. Most graphics are based on images created using dermatoscopic imaging technology. Only a few studies have been conducted on 2192 images taken in clinical or real-world settings. rash location is difficult to determine due to several issues, including: B. The pixel count is low, shadows are present, and the rash area occupies only a small part or is incomplete in the clinical or real scene image. This point requires further investigation. In the clinical detection model, an attention mechanism or target detection method can be introduced to focus on the rash site of skin diseases, which facilitates the feature extraction of the rash site and improves the accuracy of the clinical detection model.

3.4. ResNet Architecture

Residual neural networks (ResNet) are deep convolutional network that introduced in 2015 by Microsoft for visual recognition tasks and win the Large-Scale Visual Recognition Challenge (ILSVRC 2015) in image detection, classification, and localization which shows outstanding performance on the ImageNet dataset [26]. The basic idea of ResNet is to skip blocks of convolutional layers by applying shortcut connections. The fundamental blocks called "bottleneck" blocks following two rules:

- For the identical output feature map size, the layers have the same number of filters, and
- Have doubled filters if the feature map size is halved.

The down-sampling is applied directly by convolutional layers with a stride of 2, and batch normalization is applied directly after every convolution and before ReLU activation. When the input and output are of the same size, the identity shortcut is utilized. When the dimensions increase, the projection shortcut is using to match dimensions for 1 x 1 convolutions. In both cases, when the shortcuts connections go across feature maps of two sizes, they are applied with a stride of 2. Finally, the network ends with a 1000 fully connected layer with SoftMax activation. There are 50 weighted layers, with a total of 23 534 592 trainable parameters. Deep Residual Features (DRF) extracted from the latest convolutional layer of this network is also presented. Key: The notation k × k, n in the convolutional layer indicates a size k and n channels filter. FC 1000 indicates the fully connected layer with 1000 neurons. The number on the top of the convolutional layer block describes the repetition of each part. n-Classes represent the number of output classes.

3.5. VGG-16

VGG-16 is a network architecture presented by the Visual Geometric Group with 16 layers. The trainable parameters are included in these layers, and there are other layers, such as the Max-pool layer, but there are no trainable parameters. This algorithm won the 2014 Visual Recognition Challenge, i.e., Simonyan and Zisserman created ILSVRC-2014. The Lower layers of the VGG_16 can be divided into five uniform blocks. Each block has several convolutional layers with a ReLU activation function and a max-pooling layer that reduces dimensionality. The blocks of lower layers are followed by 3 fully connected layers and a SoftMax layer that performs classification.

3.6. VGG-19

VGG-19 model is different from VGG-16, just in the depth of layers. The VGG-19 contains 3 layers more compared to VGG-16. These layers learn detailed patterns of images for practical training. In earlier research, it has been observed that by applying multi-scale testing, VGG-16 decreased the error rate from 8.8% to 8.7%; likewise, VGG-19 decreased the error rate from 8.7% to 8.6%.

3.7. Training

Our models were implemented utilizing TensorFlow deep learning framework. For optimization of the neural network, Adam optimization has been applied. We adapted a dynamic learning rate which was divided by 10, every 10 epochs with an initial value of 5x10−5 and 1x10−4 in ResNet, VGG-16, and VGG-19 experiments, respectively. We used pre-trained weights on ImageNet for the convolutional blocks to initialize the network parameters, which resulted in a faster convergence (in less than 50 epochs). The training batch size was 32 images for all models.

We applied weighted cross-entropy, a modified formula of the well-known loss function - cross-entropy, to mitigate the effect of dataset imbalance. Weighted cross-entropy takes the following form:

$$H(p,q)=-WiΣxp\ (x)\ logq(x)\ldots\ldots\ldots\ldots \quad (27)$$

Where: p(x) is the ground truth label, q(x) indicates the predicted SoftMax probability of the neural network, and wi indicate weight for class i.

Furthermore, the data augmentation module has been applied to our images to train the models with various input images and artificially enlarged Dataset. Data augmentation results have been practically shown to reduce network overfitting and improve the classifiers to generalize accurately. In our work, the selected augmentation techniques were vertical flipping with a probability of 0.5, horizontal flipping with another probability of 0.5, image rotations with a probability of 0.8 applying a random aspect in the range [–25, 25], and random zooming factor in the range of [0.7, 1.3] with a probability of 0.8.

3.8. Experimental Results

In our experiments, the images were divided randomly into training, validation, and test sets with a 70/20/10% split, respectively. The validation set was utilized to determine the best epoch for the validation score. We also assess the validation results of standalone models and the ensemble of the three approaches. The ensemble is calculated by averaging the output probabilities of the three networks and choosing the class with the highest probability. Each sample in our dataset was classified into one of the two classes: chickenpox (positive) and non-chickenpox(negative). On each epoch, we calculated three commonly used metrics to evaluate our approach: accuracy, precision, and recall which are defined as follows: Our results for the validation set, test set are presented in Table 2, Table 3, respectively.

Table 2 Validation results of three approach

Method	Average Accuracy	Average precision	Average recall
ResNet	89%	84%	83%
VGG-16	91%	87%	85%
VGG-19	90%	88%	84%
Ensemble	94%	90%	87%

Table 3 Test result of ensemble learning

Method	Average Accuracy	Average precision	Average recall
Ensemble	93%	89%	85%

4. Discussion

To verify our results, we manually analyzed some misclassified images. Fig. 1a presents an example of a false positive prediction, whereas Fig. 1b an example of a false negative sample. The left photo shown in Fig. 1a is a mouth measles rash, misclassified by the model as a HFMD rash. This example presents the difficulty of distinguishing the HFMD rash from other skin diseases. Fig. 1b on the right presents sample images of HFMD that were misclassified as normal skin. Since many incorrect identifications occurred on images resembling the HFMD rash, like those of scabies and measles, it's crucial to include training images of both HFMD and these similar conditions to minimize such errors. To further illustrate the difficulty of classification, we present a couple of sample images that were correctly classified by the Convolution Neural Network (see Fig. 1a, Fig.1b). In contrast to Fig. 1a and 1b, a correctly identified HFMD image of the mouth is shown in Fig. 1c and a non-HFMD case of the hand is shown in Fig. 1d. Most cases of HFMD mainly affect the hands (Fig. 1a and 1b), the foot, or the mouth (Fig. 1a and 1b).

However, the rashes can appear in other parts of the body as well, such as on the leg, as shown in Fig. 1e and Fig. 1f. As presented in these images though, these HFMD cases of the leg were misclassified as scabies and measles, respectively. To rectify such problems, more skin rash data will need to be collected. With the spread of the chickenpox virus

increasing globally and fewer healthcare providers can correctly recognize it due to its rarity in recent decades, an accurately trained algorithm capable of distinguishing chickenpox rash is crucial in combatting the outbreak.

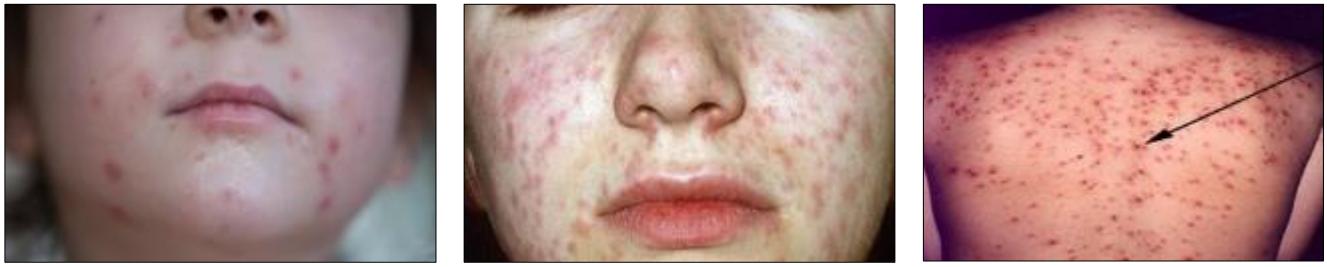

A B C

Figure 2 Three images sample that have been misclassified by separate deep convolutional neural networks but correctly classified by Ensemble method. (a) ResNet-50 classification: chickenpox, VGG-16 classification: chickenpox, ensemble classification: HFMD. (b) VGG-16 classification: chickenpox, ResNet classification: chickenpox, ensemble classification: Measles. (c) VGG-16 classification: Scabies, ResNet classification: measles, ensemble classification: chickenpox

Future work

Based on the high accuracy of 94% obtained, the proposed approach was found to be reliable. Moreover, it can be implemented in educational institutions, schools, or any other setting where students gather and skin diseases are likely to spread without requiring the presence of specialized medical personnel. Future research can be conducted in collaboration with the medical community to learn more about infectious diseases that could spread among children. To help detect diseases without the need for medical sector intervention, data from the medical sector will be gathered and integrated into an Internet of Things (IOT) system as a smart building.

5. Conclusion

In summary, our ensemble-based deep learning method, incorporating VGG-16, VGG-19, and ResNet-50 architectures, outperforms previous approaches in accurately detecting chickenpox. This advancement promises improved healthcare efficiency, aiding global efforts to combat infectious diseases and paving the way for enhanced automated diagnosis, thereby benefiting society's overall health outcomes and guiding future research towards addressing emerging healthcare challenges.

Compliance with ethical standards

Disclosure of conflict of interest

The authors have no any conflict of interest for publishing this article.

References

[1] Lanera C, Berchialla P, Baldi I, Lorenzoni G, Tramontan L, Scamarcia A, Cantarutti L, Giaquinto C, Gregori D. Use of Machine Learning Techniques for Case-Detection of Varicella Zoster Using Routinely Collected Textual Ambulatory Records: Pilot Observational Study. JMIR Med Inform. 2020 May 5;8(5): e14330. doi: 10.2196/14330. PMID: 32369038; PMCID: PMC7238079.

[2] Chae S, Kwon S, Lee D. Predicting Infectious Disease Using Deep Learning and Big Data. Int J Environ Res Public Health. 2018 Jul 27;15(8):1596. doi: 10.3390/ijerph15081596. PMID: 30060525; PMCID: PMC6121625.

[3] Oyola, J.F., Arroyo, V., Ruedin, A.M., & Acevedo, D. Detection of Chickenpox Vesicles in Digital Images of Skin Lesions. Iberoamerican Congress on Pattern Recognition. 2012 Sep, , 18 (1), pp 43– 66.

[4] National Center for Immunization and Respiratory Diseases (NCIRD) [Internet]. Baltimore: Johns Hopkins University; © 2024 [cited 2024 Jan 24]. Available from https://www.cdc.gov/chickenpox/about/symptoms.

[5] Breuer J, Fifer H. Chickenpox. BMJ Clin Evid. 2011 Apr 11; 2011:0912. PMID: 21486500; PMCID: PMC3275319.

[6] Poonam Sachdev Chickenpox Research Institute [Internet]. Baltimore: Johns Hopkins University; © 2023 [cited 2024 Jan 14]. Available from https://www.webmd.com/children/what-is-chickenpox.

[7] Mohammed, Z.F., Abdulla, A.A. An efficient CAD system for ALL cell identification from microscopic blood images. 2012 Apr, Appl 80, 6355–6368. https://doi.org/10.1007/s11042-020-10066-6.

[8] Dick V, Sinz C, Mittlböck M, Kittler H, Tschandl P. Accuracy of Computer-Aided Diagnosis of Melanoma: A Meta-analysis. JAMA Dermatol. 2019 Nov 1;155(11):1291-1299. doi: 10.1001/jamadermatol.2019.1375. PMID: 31215969; PMCID: PMC6584889.

[9] Aerts HJ, Velazquez ER, Leijenaar RT, Parmar C, Grossmann P, Carvalho S, Bussink J, Monshouwer R, Haibe-Kains B, Rietveld D, Hoebers F, Rietbergen MM, Leemans CR, Dekker A, Quackenbush J, Gillies RJ, Lambin P. Decoding tumour phenotype by noninvasive imaging using a quantitative radiomics approach. Nat Commun. 2014 Jun 3;5:4006. doi: 10.1038/ncomms5006. Erratum in: Nat Commun. 2014;5:4644. Cavalho, Sara [corrected to Carvalho, Sara]. PMID: 24892406; PMCID: PMC4059926.

[10] Esteva A, Kuprel B, Novoa RA, Ko J, Swetter SM, Blau HM, Thrun S. Dermatologist-level classification of skin cancer with deep neural networks. Nature. 2017 Feb 2;542(7639):115-118. doi: 10.1038/nature21056. Epub 2017 Jan 25. Erratum in: Nature. 2017 Jun 28;546(7660):686. PMID: 28117445; PMCID: PMC8382232.

[11] Lee H, Tajmir S, Lee J, Zissen M, Yeshiwas BA, Alkasab TK, Choy G, Do S. Fully automated deep learning system for bone age assessment. Journal of digital imaging. 2017 Aug;30:427-41.

[12] Vandenberghe ME, Scott ML, Scorer PW, Söderberg M, Balcerzak D, Barker C. Relevance of deep learning to facilitate the diagnosis of HER2 status in breast cancer. Scientific reports. 2017 Apr 5;7(1):45938.

[13] Kermany DS, Goldbaum M, Cai W, Valentim CC, Liang H, Baxter SL, McKeown A, Yang G, Wu X, Yan F, Dong J. Identifying medical diagnoses and treatable diseases by image-based deep learning. cell. 2018 Feb 22;172(5):1122-31.

[14] Ballerini L, Fisher RB, Aldridge B, Rees J. A color and texture based hierarchical K-NN approach to the classification of non-melanoma skin lesions. Color medical image analysis. 2013:63-86.

[15] Gilmore S, Hofmann-Wellenhof R, Soyer HP. A support vector machine for decision support in melanoma recognition. Experimental dermatology. 2010 Sep;19(9):830-5.

[16] Matsunaga K, Hamada A, Minagawa A, Koga H. Image classification of melanoma, nevus and seborrheic keratosis by deep neural network ensemble. arXiv preprint arXiv:1703.03108. 2017 Mar 9.

[17] Nasr-Esfahani E, Samavi S, Karimi N, Soroushmehr SM, Jafari MH, Ward K, Najarian K. Melanoma detection by analysis of clinical images using convolutional neural network. In2016 38th Annual International Conference of the IEEE Engineering in Medicine and Biology Society (EMBC) 2016 Aug 16 (pp. 1373-1376). IEEE.

[18] Majtner T, Yildirim-Yayilgan S, Hardeberg JY. Combining deep learning and hand-crafted features for skin lesion classification. In2016 Sixth International Conference on Image Processing Theory, Tools and Applications (IPTA) 2016 Dec 12 (pp. 1-6). IEEE.

[19] Kwasigroch A, Mikołajczyk A, Grochowski M. Deep neural networks approach to skin lesions classification—A comparative analysis. In2017 22nd international conference on methods and models in automation and robotics (MMAR) 2017 Aug 28 (pp. 1069-1074). IEEE.

[20] Stolz WJ. ABCD rule of dermatoscopy: a new practical method for early recognition of malignant melanoma. Eur J Dermatol. 1994;4:521-7.

[21] Argenziano G, Fabbrocini G, Carli P, De Giorgi V, Sammarco E, Delfino M. Epiluminescence microscopy for the diagnosis of doubtful melanocytic skin lesions: comparison of the ABCD rule of dermatoscopy and a new 7-point checklist based on pattern analysis. Archives of dermatology. 1998 Dec 1;134(12):1563-70.

[22] Soyer HP, Argenziano G, Zalaudek I, Corona R, Sera F, Talamini R, Barbato F, Baroni A, Cicale L, Di Stefani A, Farro P. Three-Point Checklist of DermoscopyA New Screening Method for Early Detection of Melanoma. Dermatology. 2004 Jul 1;208(1):27-31.

[23] Henning JS, Dusza SW, Wang SQ, Marghoob AA, Rabinovitz HS, Polsky D, Kopf AW. The CASH (color, architecture, symmetry, and homogeneity) algorithm for dermoscopy. Journal of the American Academy of Dermatology. 2007 Jan 1;56(1):45-52.

[24] Velasco J, Pascion C, Alberio JW, Apuang J, Cruz JS, Gomez MA, Molina Jr B, Tuala L, Thio-ac A, Jorda Jr R. A smartphone-based skin disease classification using mobilenet cnn. arXiv preprint arXiv:1911.07929. 2019 Nov 13.

[25] G. Rezende, T. Ruppert, F. Carvalho, P. Ramos, and de, Geus, "Malicious Software Classification Using Trans-fer Learning of ResNet-50 Deep Neural Network," 16th IEEE International Conference on Machine Learning and Applications (ICMLA), pp. 1011-1014, doi: 10.1109/ICMLA.2017.00-19, 2017.

[26] Mahmood A, Ospina AG, Bennamoun M, An S, Sohel F, Boussaid F, Hovey R, Fisher RB, Kendrick GA. Automatic hierarchical classification of kelps using deep residual features. Sensors. 2020 Jan 13;20(2):447.

[27] Shahin AH, Kamal A, Elattar MA. Deep ensemble learning for skin lesion classification from dermoscopic images. In2018 9th Cairo International Biomedical Engineering Conference (CIBEC) 2018 Dec 20 (pp. 150-153). IEEE.